OPTO-ELECTRONICS REVIEW 9(4), 385–390 (2001)

Relationship between deep levels and R_0A product in HgCdTe diodes

S.K. SINGH[1], V. GOPAL*[1], and R.M. MEHRA[2]

[1]Solid State Physics Laboratory, Lucknow Road, Timarpur, Delhi, 110054, India
[2]Department of Electronic Science, University of Delhi South Campus Delhi, 110054, India

This paper presents an analysis of the recently reported data of Yoshino et. al. [1,2] on p⁺-n HgCdTe diodes with a view to verify quantitatively the previously reported relationship between deep levels and R_oA product of the diodes. The result of this analysis suggests that the trap level, located below 6 meV from the bottom of the conduction band edge, contributes to the trap assisted tunnelling currents in the medium reverse bias region. Also there is evidence that zero bias resistance area product is limited by the ohmic surface leakage and generation-recombination contributions. The observed current-voltage (I–V) characteristics and dynamic resistance-voltage (R_d–V) characteristics have been shown to excellently fit the theory by taking into account the contributions due to: (i) thermal diffusion of minority carrier from the neutral regions, (ii) generation–recombination (g-r) current in the depletion region, (iii) trap assisted tunnelling (TAT) currents due to a trap level located at 6 meV below the bottom of the conduction band edge, (iv) band to band tunnelling (BTB) currents, and (v) ohmic component of surface leakage currents.

Though the R_oA product of the diodes is shown to be limited by g-r and surface concentrations, the variation in R_oA product of the diodes is interpreted as arising due to the variation in planar area of the diodes accompanied with the varying surface contributions, since g-r contribution should remain constant for all diodes.

Keywords: HgCdTe, R_oA product, trap levels, p⁺-n diode

1. Introduction

The relationship between the figure of merit R_oA representing the junction property and deep levels representing electrical properties of semiconductor HgCdTe material have been recently reported by Yoshino *et. al.* [1,2]. These authors estimated the R_oA product of the mesa etched p⁺-n HgCdTe diode from I–V characteristics and the deep levels from the spectral analysis of deep level transient spectroscopy (SADLTS). In this way the relationship between deep levels and R_oA product could be concluded only qualitatively, since no attempt was made to quantitatively verify the contribution of deep levels to the I–V and R_d–V characteristics of the diodes with the observed levels from the SADLTS measurements. In this paper, we are attempting to quantitatively correlate I–V and R_d–V characteristics of the diodes with the deep levels reported from SADLTS measurements.

2. Model

It has been recently reported that the density of traps contributing to the trap assisted tunnelling currents in an n⁺-p HgCdTe diode can be estimated from the analysis of the dynamic resistance variation in the reverse bias characteristic of the given diode [3]. In the present paper, we make use of the same approach to estimate the density of traps and their location in the band gap in case of p⁺-n HgCdTe diodes, too. Since we are analysing the reverse bias characteristics, it will be assumed that one of the dark current components is due to the trap assisted tunnelling of holes (minority carrier) from the n-side of the junction [4,5]. The other dark current components are: the thermal diffusion of minority carriers from the neutral regions, g-r current in the depletion region, band to band tunnelling currents and surface leakage current due to shunt resistance. The relevant expressions describing each of these current components and the associated dynamic resistances are briefly summarised below.

2.1. Diffusion current (I_{dif})

The thermal diffusion of minority carriers (i.e. electrons) from the p⁺ side of junction being negligible will be ignored. The major contribution (i.e., diffusion of holes) is from the n- side and is described by the following well-known equation [6,7]

$$I_{dif} = \left[\frac{qAn_i^2}{N_d}\left\{\frac{kT}{q}\frac{\mu_h}{\tau_h}\right\}^{1/2}\right]\tanh\frac{d}{L_p}\left(\exp\left(\frac{qV}{kT}\right)-1\right), \quad (1)$$

where N_d is the donor concentration, n_i is the intrinsic carrier concentration, A is the junction area, V the diode bias

*e-mail: vishnu_gopal/sspl@ssplnet.org

voltage, d the thickness of the n-region, τ_h the hole lifetime and μ_h hole mobility. The above equation can be rewritten as

$$I_{dif} = \frac{kT}{qR_{odif}}\left[\exp\left(\frac{qV}{kT}\right)-1\right], \tag{2}$$

where R_{odif} is the diffusion limited resistance. Since the lifetime and mobility in the sample under study is not known so we will use the above equation to calculate the diffusion current contribution. The values of R_{odif} used for calculating the diffusion contribution are given in Table 1. The associated dynamic resistance and its derivatives are given by

$$R_{dif}^{-1} = \frac{1}{R_{odif}}\exp\left(\frac{qV}{kT}\right), \tag{3}$$

$$\frac{\partial I_{dif}}{\partial V^2} = \frac{q}{kT}\frac{1}{R_{odif}}\exp\left(\frac{qV}{kT}\right). \tag{4}$$

2.2. Generation recombination current (I_{gr})

In this type of current, defects within the depletion region acting as intermediate states for the thermal generation and recombination of carriers. The resulting generation-recombination (g-r) current is calculated by using simplified expression [8,9]

$$I_{gr} = \frac{qn_iW_{dep}A}{2\tau_{gr}}\left[\exp\left(\frac{qV}{2kT}\right)-1\right], \tag{5}$$

where τ_{gr} is the g-r lifetime (in the present paper for calculating the g-r contribution 350 ns lifetime is chosen) and W_{dep} is the voltage dependent depletion region width given by

$$W_{dep} = \left[\frac{2\varepsilon_o\varepsilon_sV_t(N_a+N_d)}{qN_aN_d}\right]^{1/2}, \tag{6}$$

where $V_t = V_{bi} + V$ is the total junction potential, ε_o is the permittivity of free space, ε_s is the static dielectric constant of HgCdTe. The g-r current can be rewritten as

$$I_{gr} = A_{gr}V_t^{1/2}\left[\exp\left(\frac{qV}{2kT}\right)-1\right],$$
$$A_{gr} = \frac{qn_iA}{2\tau_{gr}}\left[\frac{2\varepsilon_o\varepsilon_s(N_a+N_d)}{qN_aN_d}\right]^{1/2}, \tag{7}$$

where A_{gr} is the voltage independent term in Eq. (7). The associated dynamic resistance and its derivatives are given by

$$R_{gr}^{-1} = A_{gr}\left[\frac{1}{2}V_t^{-1/2}\left\{\exp\left(\frac{qV}{2kT}\right)-1\right\}+\left(-\frac{q}{2kT}\right)V_t^{1/2}\exp\left(\frac{qV}{2kT}\right)\right], \tag{8}$$

$$\frac{\partial I_{gr}}{\partial V^2} = A_{gr}\left[-\frac{1}{4}V_t^{-3/2}\left\{\exp\left(\frac{qV}{2kT}\right)-1\right\}\frac{q}{2kT}V_t^{-1/2}\exp\left(\frac{qV}{2kT}\right)+\left(\frac{q}{2kT}\right)^2V_t^{1/2}\exp\left(\frac{qV}{2kT}\right)\right]. \tag{9}$$

2.3. Trap assisted tunnelling current (I_{tat})

In this type of current, minority carriers may tunnel from the occupied trap states on the quasi neutral side to the empty bands states on the other side of the junction [3], or through trap sites present in the depletion region of the junction [5,6]. In p^+-n junctions, the major contribution of the trap assisted tunnelling may be due to tunnelling of holes, via trap levels to valence band on the p-side which is completely analogous to the tunnelling of electrons via trap levels to conduction band on the n-side in case of n^+-p diodes [4]. This current is being calculated using a modified simple one-dimensional model [10]

$$I_{tat} = qAN_tW_{dep}W_vN_v, \tag{10}$$

where W_vN_v, the tunnelling rate of holes are given in Refs. 5 and 6.

$$W_vN_v = \frac{\pi^2qm_vEM^2}{h^3(E_g-E_t)}\exp\left\{\left(\frac{4(2m_v)^{1/2}(E_g-E_t)^{3/2}}{3q\hbar E}\right)\right\}, \tag{11}$$

Table 1. Diode parameters.

Diode No.	Diode size (μm)	R_{odif} (Ω)	R_o (Ω)	R_oA (Ω cm^2)	Estimated N_t (cm^{-3})	Estimated R_{sh} (Ω)
1	150	1.00×10^7	9.62×10^5	216	1.250×10^{14}	1.4×10^6
2	150	1.00×10^7	5.28×10^5	118	5.217×10^{14}	2.6×10^6
3	50	9.00×10^7	4.09×10^6	102	1.390×10^{15}	1.2×10^7
4	100	2.25×10^7	1.50×10^6	150	2.670×10^{14}	2.3×10^6

$$T_p = \exp\left[-\left(\frac{2m_e}{\hbar^2}\right)^{1/2}\left(\frac{2\varepsilon_o\varepsilon_s}{q^2N_d}\right)^{1/2} E_g\left\{\left(1-\frac{E}{E_g}\right)\left[\frac{\pi}{2}-\sin^{-1}\left(\frac{-E}{E_g-E}\right)^{1/2}\right]-\left(-\frac{E}{E_g}\right)^{1/2}\right\}\right], \quad (16)$$

where m_v is the effective mass of carrier in the valence band, E_g is the band gap, M is the matrix element associated with the trap potential, h is the Planck's constant, E is the electric field strength across the depletion region, and E_t is the position of trap levels in the band gap measured from the bottom of the conduction band on the n side. Since the tunnelling rate of carriers is inversely proportional to the exponent of their mass, the tunnelling probability of heavy hole is much smaller than that of light holes. As a result, the hole tunnel transition is dominated by light holes. As reported by the earlier authors, we assume the value of the quantity $M^2(m_v/m)$ as 10^{-23} Vcm^3 for HgCdTe [5,6].

The associated dynamic resistance and its derivatives are given by

$$(R_{tat})^{-1} = \frac{2q^3A\pi^2m_vM^2}{h^3(E_g-E_t)} N_t \exp\left(-\frac{B}{V_t^{1/2}}\right)\left(1+\frac{B}{2V_t^{1/2}}\right), \quad (12)$$

$$\frac{\partial I_{tat}}{\partial V^2} = \frac{2q^3A\pi^2m_vM^2}{h^3(E_g-E_t)} N_t \exp\left(-\frac{B}{V_t^{1/2}}\right)\left(\frac{B}{4V_t^{3/2}}+\frac{B^2}{4V_t^2}\right), \quad (13)$$

$$B = \frac{4(2m_e)^{1/2}(E_g-E_t)^{3/2}}{\left\{3q\hbar\left(\frac{2qN_d}{\varepsilon_o\varepsilon_s}\right)^{1/2}\right\}}, \quad (14)$$

where B, depends on the shape of the barrier and for a triangular barrier it's value is given in Eq. (14), and N_t is the density of traps occupied by holes.

2.4. Band to band tunnelling current (I_{btb})

At relatively higher bias voltages, the electrons directly tunnelling from the valance band on the p^+ side to the to the conduction band on the n-side are responsible for the BTB current [11,12]. For modelling this current we use the simple approach presented in Ref. 11. The band-to-band tunnelling current is given by

$$I_{btb} = \frac{qA}{4\hbar\pi^2}\left\{\frac{E_gkT}{P^2}\right\}^{1/2} \int_{-E_{max}}^{0} T_p\left(\frac{E}{2}\right)dE, \quad (15)$$

where $E_{max} = -qV + E_f$, P is the momentum matrix element and E_f the fermi energy. T_p is the tunnelling probability associated with the band to band tunnelling and is given by

The associated dynamic resistance and its derivatives are given by

$$(R_{btb})^{-1} = \left(\frac{q^2A}{4\hbar\pi^2}\right)\left(\frac{E_gkT}{P^2}\right)T_p\left(\frac{E_{max}}{2}\right), \quad (17)$$

$$\frac{\partial^2 I_{btb}}{\partial V^2} = \left(\frac{q^3A}{4\hbar\pi^2}\right)\left(\frac{E_gkT}{P^2}\right)\left(\frac{2m_e}{\hbar^2}\right)^{1/2}\left(\frac{2\varepsilon_o\varepsilon_s}{q^2N_d}\right)^{1/2} \times \quad (18)$$

$$\times E_gT_p\left(\frac{E_{max}}{2}\right)\left[-\frac{\pi}{2E_g}+\frac{\sin^{-1}\left(\frac{-E}{E_g-E}\right)^{1/2}}{E_g}\right].$$

2.5. Surface leakage current (I_{sh})

The current voltage characteristics of a mercury cadmium telluride junction often exhibit an excess current known as surface leakage current. This component of current can be modelled as an ohmic current component given in Ref. 13

$$I_{sh} = \frac{V}{R_{sh}}, \quad (19)$$

where V is the applied voltage across the junction and R_{sh} is the diode shunt resistance.

3. Analytical method

The above stated currents will be now used for the modelling of current-voltage characteristics and dynamic resistance variation with the reverse bias voltage of the HgCdTe diodes. To analyse the given experimental data, the density of trap levels participating in the tunnelling process can be first estimated from the position of the observed maxima (V_m) in the dynamic resistance versus reverse bias voltage plot by applying the following condition

$$\frac{\partial R}{\partial V} = 0, \quad (20)$$

where R is the resultant dynamic resistance given by

$$\frac{1}{R} = \frac{1}{R_{dif}} + \frac{1}{R_{gr}} + \frac{1}{R_{tat}} + \frac{1}{R_{btb}} + \frac{1}{R_{sh}}, \quad (21)$$

The trap density is obtained from mathematical manipulation of Eqs. (4), (9), (13), (18), (20) and (21), which is given by

$$N_t = \frac{\left\{\left(\frac{\partial^2 I_{dif}}{\partial V^2}\right)_{V=V_m} + \left(\frac{\partial^2 I_{gr}}{\partial V^2}\right)_{V=V_m} + \left(\frac{\partial^2 I_{btb}}{\partial V^2}\right)_{V=V_m}\right\}}{\frac{2q^3 A\pi^2 m_v M^2}{h^3(E_g - E_t)} \exp\left(-\frac{B}{V_m^{1/2}}\right)\left(\frac{B}{4V_m^{3/2}} + \frac{B^2}{4V_m^2}\right)}, \quad (22)$$

For a given material of known composition, all the parameters on the RHS of Eq. (22) are known. Note that above estimate of N_t is practically independent of surface leakage current contribution, since $\partial R_{sh}/\partial V = 0$ (shunt resistance R_{sh} is independent of applied voltage V). This situation further allow us to obtain an estimate of the shunt resistance R_{sh} from a comparison of experimentally determined peak dynamic resistance and theoretically calculated dynamic resistance from the combined contribution of BTB, TAT (making use of estimated N_t), g-r current and thermal diffusion currents.

4. Application to the experimental data

To investigate the relationship between deep levels observed from SADLTS measurements and R_oA product in HgCdTe diodes, we now make use of model described in the previous section to analyse the experimental data of Yoshino *et. al.* in Refs. 1 and 2. To begin with it was assumed that only a single trap level is participating in the tunnelling process. The model described above was then used to estimate N_t and shunt resistance of each diode from the position of peak dynamic resistance by varying the position of trap level. As shown in Fig. 1, it is interesting to observe that the experimental data of all the four diodes can be fitted very well with the model described here by assuming that a single trap level located at 6 meV below the bottom of the conduction band edge contribute to trap assisted tunnelling current in addition to the thermal diffusion cur-

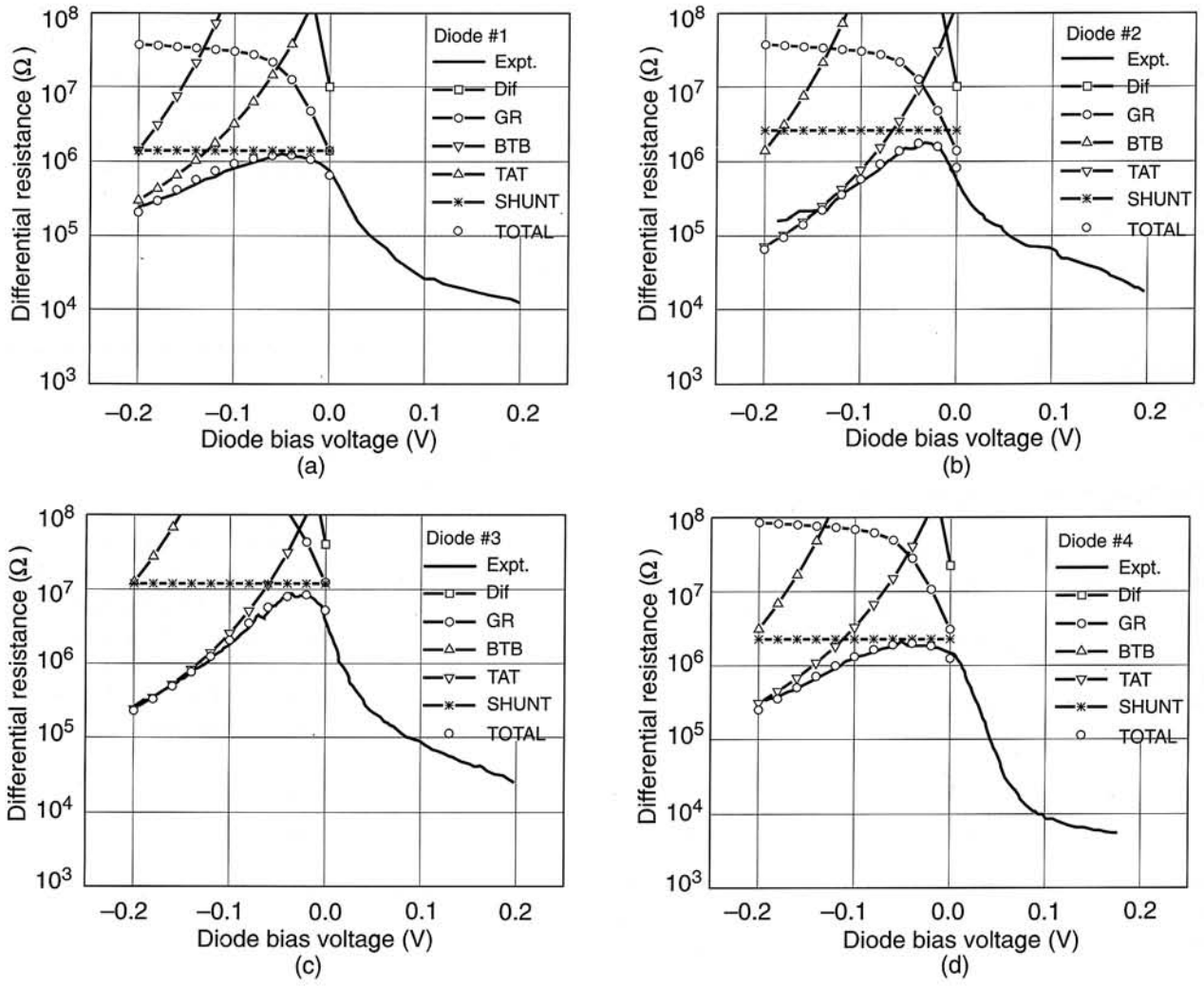

Fig. 1. Comparison of experimental (continuous line curve) and theoretically (discrete points) calculated variation of dynamic resistance in reverse bias region. The relative contributions of different current mechanisms to the total dynamic resistance are also shown.

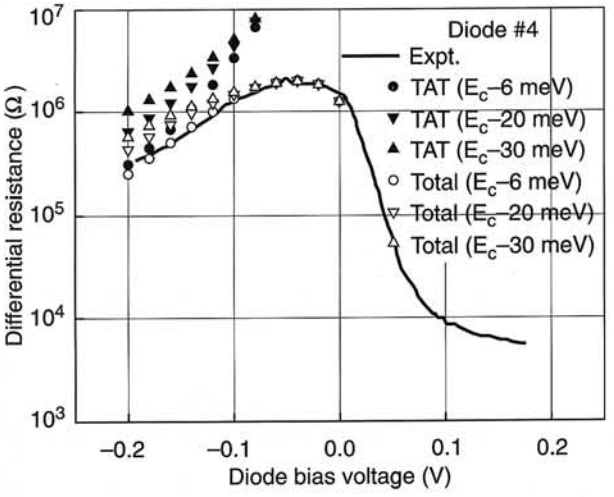

Fig. 2. Comparison of the trap assisted tunnelling contribution (shown by filled discrete points) to the dynamic resistance (open discrete points) due to different trap levels E_c–20 meV, E_c–30 meV as against the E_c–6 meV levels. Results for the other diode numbers (1–3) was also similar.

rent, g-r current, band to band tunnelling and shunt surface leakage currents. The value of each of the estimated parameters N_t and R_{sh} are shown in Table 1 for comparison. For the sake of completeness we show in Fig. 2, a comparison of the trap assisted tunnelling contribution (shown by filled discrete points) to the dynamic resistance (open discrete points) due to deep levels E_c–20 meV, E_c–30 meV as against the E_c–6 meV levels. It is observed that the contribution due to deeper levels at 20 meV and 30 meV is relatively very small. In other words, we can say that shallow level at 6 meV is the dominant level, which participates in the trap-assisted tunnelling process and contribute to the dynamic resistance of the diode in medium and higher reverse bias region.

Coming to the variations in R_oA product of the diodes, it can be noted from Fig. 1 that the combination of ohmic surface shunt resistance and g-r resistance limits the zero bias resistance of the diode. The contributions either due to TAT or BTB have negligible influence on the zero bias resistance. One notes from Table 1 that diode #1 and diode #2 are having different R_oA in spite of same area. It can be understood from Fig. 1. Note that g-r contribution is higher to the zero bias dynamic resistance of diode #2 than diode #1. In the calculation of g-r current it is assumed that the mid gap levels contributes to the g-r current, the participation of deep levels at E_c–30 meV which is located towards the midgap region contributing to the g-r current cannot be therefore completely ruled out.

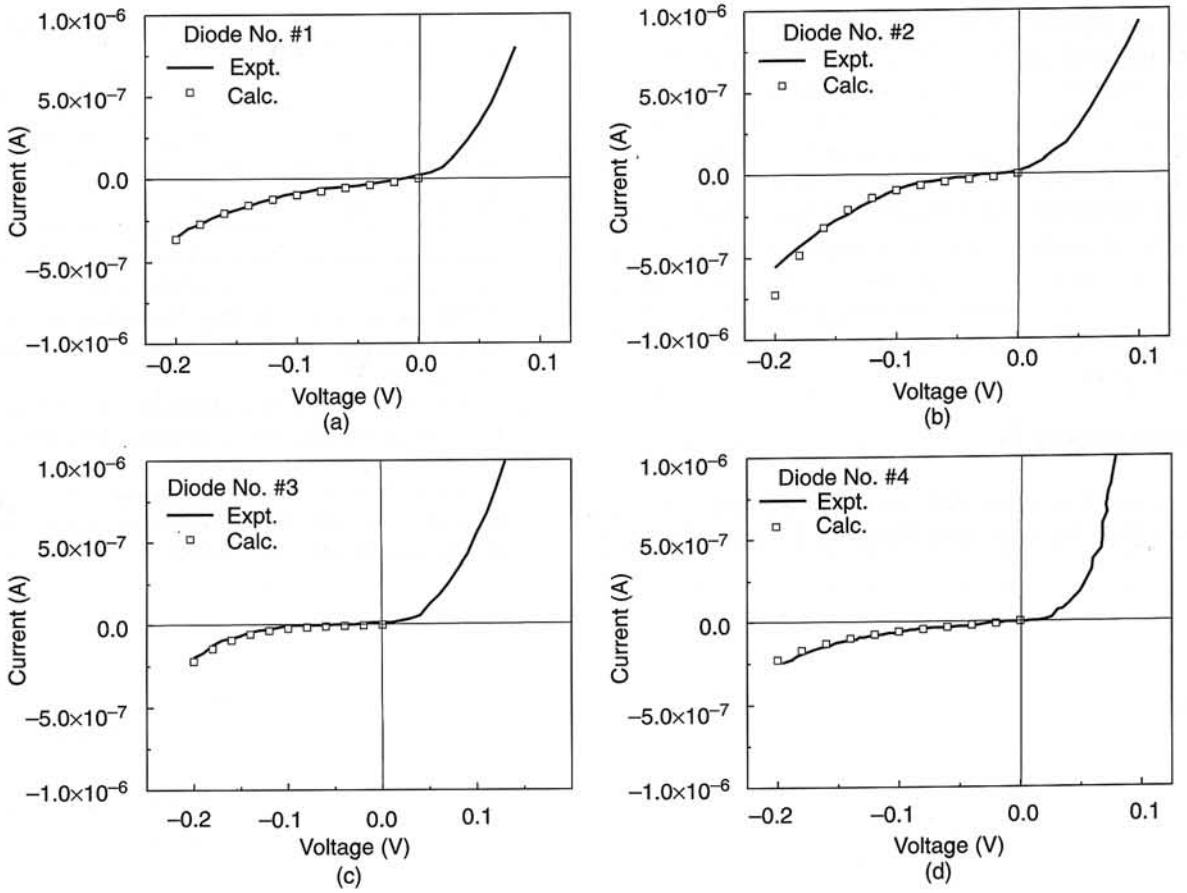

Fig. 3. Comparison of experimental (continuous line curve) and theoretically calculated current voltage characteristics in the reverse bias region.

Besides the agreement of R_d–V characteristics of diodes with the theory, Fig. 3 shows the agreement for I–V characteristics too. The excellent agreement between theory and experimental data in case of both I–V and R_d–V characteristics of each diode coupled with the reasonable estimates of the trap density in each case led us to propose that the shallow level at 6 meV is dominantly responsible for affecting the diodes dynamic resistance in the reverse bias region.

It is further interesting to note from Table 1, that the estimated trap density increases with the decrease in diode size except in case of diode #2. This has led us to suggest that the traps participating in the tunnelling process may be located in the surface region since the surface contribution becomes increasingly more prominent with the reduction in the diode size due to increase in perimeter to area ratio [13]. This suggestion is quite consistent with the reported statement of Yoshino *et. al.* [1,2] that the 6 meV trap level could be due to the damage occurring on account of chemical etching or ion milling procedures used in the fabrication process of diodes during mesa structuring.

5. Conclusions

In this paper we have attempted to model the reported I–V and R_d–V characteristics of p^+-n HgCdTe mesa diodes by Yoshino *et. al.* [1,2] to verify the contribution of deep levels to the R_oA product. The results of this analysis show that of the trap levels (at E_c–6 meV, E_c–20 meV, and E_c–30 meV) observed in SADLTS measurements, the level at 6 meV contributes to the trap assisted tunnelling which influences the diodes dynamic resistance in medium and higher reverse bias region. The possibility of other two levels at E_c–20 meV and E_c–30 meV contributing to the g-r current, which have been found to influence the zero bias dynamic resistance cannot be completely ruled out, although the dominant g-r contribution comes from mid gap levels. In addition ohmic component of surface leakage current has been also found to limit the zero bias resistance of these diodes.

Acknowledgement

The authors (SKS and VG) are thankful to Prof. Vikram Kumar, Director Solid State Physics Laboratory, Delhi for the constant encouragement and granting permission to publish this paper.

References

1. J. Yoshino, J. Morimoto, H. Wada, A. Ajisawa, M. Kawano, and N. Oda, "Studies of relationship between deep levels and R_oA product in mesa type HgCdTe devices," *Opto-Eelectron. Rev.* **7**, 361–367 (1999).
2. J. Yoshino, J. Morimoto, and H. Wada, "Study of deep levels in mesa-type HgCdTe device," *Jpn. J. Appl. Phys.* **37**, 4027–4031 (1998).
3. S.K. Singh, V. Gopal, R.K. Bhan, and V. Kumar, "An analysis of the dynamic resistance variation as a function of reverse bias voltage in HgCdTe diode," *Semicond. Sci. Technol.* **15**, 752–755 (2000).
4. W.W. Anderson and H.J. Hoffman, "Field ionisation of deep levels in semiconductors with applications to $Hg_{1-x}Cd_xTe$ junction," *J. Appl. Phys.* **53**, 9130–9145 (1982).
5. D Rosenfeld and G. Bahir, "A model for the trap-assisted tunnelling mechanism in diffused n-p and implanted n^+-p HgCdTe photodiodes," *IEEE Transactions on Electron Devices* **39**, 1638–1645 (1992).
6. Y Nemirovsky, D Rosenfeld, R Adar, and A Kornfeld, "Tunnelling and dark currents in HgCdTe photodiodes," *J. Vac. Sci. Technol.* **A7**, 528–535 (1989).
7. Y Nemirovsky, R. Fastow, M Meyassed, and A. Unikovsky, "Trapping effects in HgCdTe," *J. Vac. Sci. Technol.* **B9**, 1829–1839 (1991).
8. S. Velicu, R. Ashokan, and S. Sivananthan "A model for dark current and multiplication in HgCdTe avalanche photodiodes," *J. Electronic Materials* **29**, 823–827 (2000).
9. A.R. Reisinger, F.G. Weaver, M.A. Rader, J.J. Voelker, S.J. Caputi, T.H. Myers, and J.F. Shanley, "Thermal effects in Hg diffused long wave infrared HgCdTe photodiodes," *J. Appl. Phys.* **71**, 483–488 (1992).
10. J.Y. Wong, "Effect of trap tunnelling on the performance of long-wavelength $Hg_{1-x}Cd_xTe$ photodiodes," *IEEE Transactions on Electron Devices* **27**, 48–57 (1980).
11. Y Nemirovsky and I. Bloom, "Tunnelling currents in reverse biased $Hg_{1-x}Cd_xTe$ photodiodes," *Infrared Phys.* **27**, 143–151 (1987).
12. A. Rogalski, "Photovoltaic detectors," in *Infrared Photon Detectors*, p. 56, edited by A. Rogalski, SPIE Optical Engineering Press, Bellingham, 1995.
13. V. Gopal, "Variable area diode data analysis of surface and bulk effects in HgCdTe photodetector arrays," *Semicond. Sci. Technol.* **9**, 2267–2271 (1994).

